Assessment of Trace Elements in Urban Road Dust of a City in a Border Province Concerning Their Levels, Sources, and Related Health Risks

Ibrahim H. Alsohaimi, Mohammed A. El-Hashemy, Abdullah G. Al-Ruwaili, Tarek A. Seaf El-Nasr & Nayef S. Almuaikel

Archives of Environmental Contamination and Toxicology

ISSN 0090-4341
Volume 79
Number 1

Arch Environ Contam Toxicol (2020) 79:23-38
DOI 10.1007/s00244-020-00737-8

Springer

Archives of Environmental Contamination and Toxicology (2020) 79:23–38
https://doi.org/10.1007/s00244-020-00737-8

Assessment of Trace Elements in Urban Road Dust of a City in a Border Province Concerning Their Levels, Sources, and Related Health Risks

Ibrahim H. Alsohaimi[1] · Mohammed A. El-Hashemy[1,2] · Abdullah G. Al-Ruwaili[1] · Tarek A. Seaf El-Nasr[1,3] · Nayef S. Almuaikel[1]

Received: 8 February 2020 / Accepted: 8 April 2020 / Published online: 28 April 2020

Abstract

Most research studies regarding the contamination of urban road dust (RD) focused on mega cities, but little consideration is given for small cities in border areas. The present work investigated the trace elements content in 16 RD samples of particle size < 63 µm at six areas with different anthropogenic activities in Sakaka city, KSA. The trace elements were analyzed using XRF and ICP-MS. Significantly high trace elements concentrations were recorded at small-scale industrial area. Concentrations of trace elements are ranked as Fe > Mn > Pb > Zn > Cr > Cu > Co > As > Se. The contamination evaluation through enrichment factor calculation refers to the existence of an anthropogenic source for certain trace elements, such as Fe, Zn, Mn, Cu, and Pb. The values of contamination factor indicate the contamination of RD samples collected from small-scale industrial area with these trace elements. The highest pollution load index value recorded at this industrial area suggests that it is a highly polluted area. This was confirmed by applying the one-way ANOVA test for the difference analysis between the investigated areas. The correlation between most of the detected trace elements at the small scale-industrial area was lost due to the variation in their industrial sources. The health risk of some detected trace elements was estimated for two groups of populations, namely workers at the small scale-industrial area and residents (adults and children) at residential areas at this city under study. Workers and resident children were more likely affected by arsenic through the ingestion pathway to cancer because of its higher cancer risk values that were more than the acceptable value 1×10^{-6}. Workers and residents (adults and children) are susceptible to noncarcinogenic risks through the ingestion pathway of Fe because of its higher hazard quotient values that are more than one.

Border provinces are characterized by small cities with low population and low congestion compared with central provinces with their mega cities. But these border cities have characteristic anthropogenic activities that leads to heavy metals emission into the environment. Most of these heavy metals are stored in the road dust as trace elements. One of these anthropogenic activities is the small-scale industries. This type of industries is defined as either nonmanufactured industries with no more than 20 workers and employees or manufacturing industries with less than 100 workers and employees (Seneviratne and Phoon 2006). These industries have several features, such as owned and operated independently, and controlled closely by owners or managers who are decision makers (Ahmad et al. 2017). The small-scale industries, for instance, car service, body painting, auto repairing, and metallic welding workshops, represent an urgent and indispensable need for urban residents. These industries have a key role in the booming of countries' economic growth by introducing a large proportion of jobs (Balkhyour et al. 2019). On the other hand, contaminations emitted from small-scale industries, especially particulate matter, can affect the environment, through pollutant enrichment of road dust.

Road dust (RD) is formed by the atmospheric deposition of particulate matter by the influence of gravity in road surface. This particulate matter comes from various sources, such as traffic emissions, construction processes, industrial

✉ Mohammed A. El-Hashemy
mohammed_elhashmy@yahoo.com;
maelhashemy@ju.edu.sa

[1] Chemistry Department, College of Science, Jouf University, P.O. Box 2014, Sakaka, Aljouf, Kingdom of Saudi Arabia

[2] Air Pollution Research Department, Environmental Research Division, National Research Centre, Dokki, Giza 12622, Egypt

[3] Chemistry Department, Faculty of Science, Al-Azhar University, Assuit Branch, Assuit 75124, Egypt

activities, etc. (Cao et al. 2017). Resuspension and deposition of road dust particles enable it to act as a source and a sink for both inorganic and organic pollutants, such as heavy metals and polyaromatic hydrocarbons (PAHs), respectively (Offenberg et al. 2003; Khanal et al. 2018). The danger of RD lies in its possibility of entering the aquatic environment and urban drainage networks, as well as its widespread movement through air. It was found that 10% of suspended particulates ($PM_{2.5}$) in urban environments were released from RD (Yu et al. 2013). Therefore, RD is considered one of the most dangerous sources of environmental pollutants in urban areas, which indicates the extent of the atmospheric deposition of heavy metals (Zheng et al. 2010).

Documentation of the harmful impacts of exposure to heavy metals on human health was performed satisfactorily (Valko et al. 2006; Kumar and Gayathri 2009; Zheng et al. 2006; Shyam et al. 2013, Sun et al. 2010). People exposed to high doses of trace metals suffer from various diseases, such as cardiovascular issues, osteoporosis, tumors, renal, and gastrointestinal toxicity (Vardhan et al. 2019). To reach the human body readily, there are three pathways for heavy metals: inhalation, ingestion, and dermal contact (Cook et al. 2005).

There is previous research related to the determination of trace elements content in RD and their health risks (Zheng et al. 2010; Apeagyei et al. 2011). However, most of these studies were done at mega-cities or capital cities that are characterized by high traffic due to their high population density, such as Cairo (Egypt) (Abdel-Latif and Saleh 2012), Tokyo (Japan) (Khanal et al. 2015), Jeddah (KSA) (Shabbaj et al. 2018), Dhaka (Bangladesh) (Rahman et al. 2019), and Guangzhou (China) (Liang et al. 2019). On the other hand, small cities, especially at border provinces, have little attention.

The goals of this study were to investigate the elemental composition of fine fraction of road dust gathered in Sakaka City and to evaluate the contamination levels of these elements at small-scale industries areas compared with other areas with different activities. This was done by calculating enrichment and contamination factors besides pollution load index. Finally, both trace elements carcinogenic and noncarcinogenic risks were estimated for adults and children inhabitants in addition to workers at the small-scale industrial area.

Materials and Methods

Sampling Sites

Figure 1 shows the RD sampling sites in Sakaka city, located at the northern border of KSA. It is a capital of a border province called Al-Jouf. A concise description of these sampling sites was displayed in Table 1.

Sample Collection

Samples were gathered with a smooth brush and plastic powder pan from an area of 1 m^2 from each sampling site in April 2019. The collected dust samples were separated into three equal quantities then stored in polyethylene pages.

Sample Processing

At first, drying of RD samples at 105 °C was done using an oven for 24 h and then screened through a tower consisting of seven sieve dishes whose mesh sizes were as follows: 1000, 500, 355, 250, 180 125, and less than 63 µm. They were ordered from the largest to the smallest mesh size. Due to the ability of RD particles of low volume (< 63 µm) for redispersion process (Al-Dabbous et al. 2013), the analysis of trace element content was restricted to this smaller size. For sample digestion, 5 ml of concentrated nitric acid (HNO_3) was added to 1 g of each sample. Then, the samples were boiled slowly and evaporated on a sand bath at 100 °C to the lowest possible volume (near dryness). Heating and addition of concentrated HNO_3 were continued until digestion was completed (clear solution). Digested samples were rinsed with distilled water and filtered. Finally, the filtrate was diluted to 25 ml using ultra-pure water (Eaton et al. 1995).

Instrumentation

Total metal contents were measured in road dust samples by using x-ray fluorescence spectrometry (XRF-1800, Shimadzu, Japan) with a rhodium (Rh) x-ray tube with a 4.0 kW thin-window x-ray tube generator (40 kV, 95 mA), using fundamental parameter (FP) method. Calibration curve method (linear and quadratic) in addition to automatic selection of five divisions (Ti-U; S, K, Ca, Sn-Cs; S; Si and Al) were performed. RD samples were mechanically compressed to make pellets for x-ray fluorescence (XRF) analysis in form of quantitative and qualitative analysis mode. The obtained results are in terms of weight percentage.

Analysis of digested samples was done using Inductively Coupled Plasma ICP-MS (Agilent 7500CE). Three replicates of each sample were measured. The tested solutions were continuously aspirated at 5 ml min^{-1}. Reference standards (supplied from Agilent Co.) of each metal (1000 mg L^{-1}) were used. The detection and quantification limits of this method for the desired trace elements (Fe, Cr, Mn, Co, As, Se, Zn, Pb, Cu) are listed in Table 2.

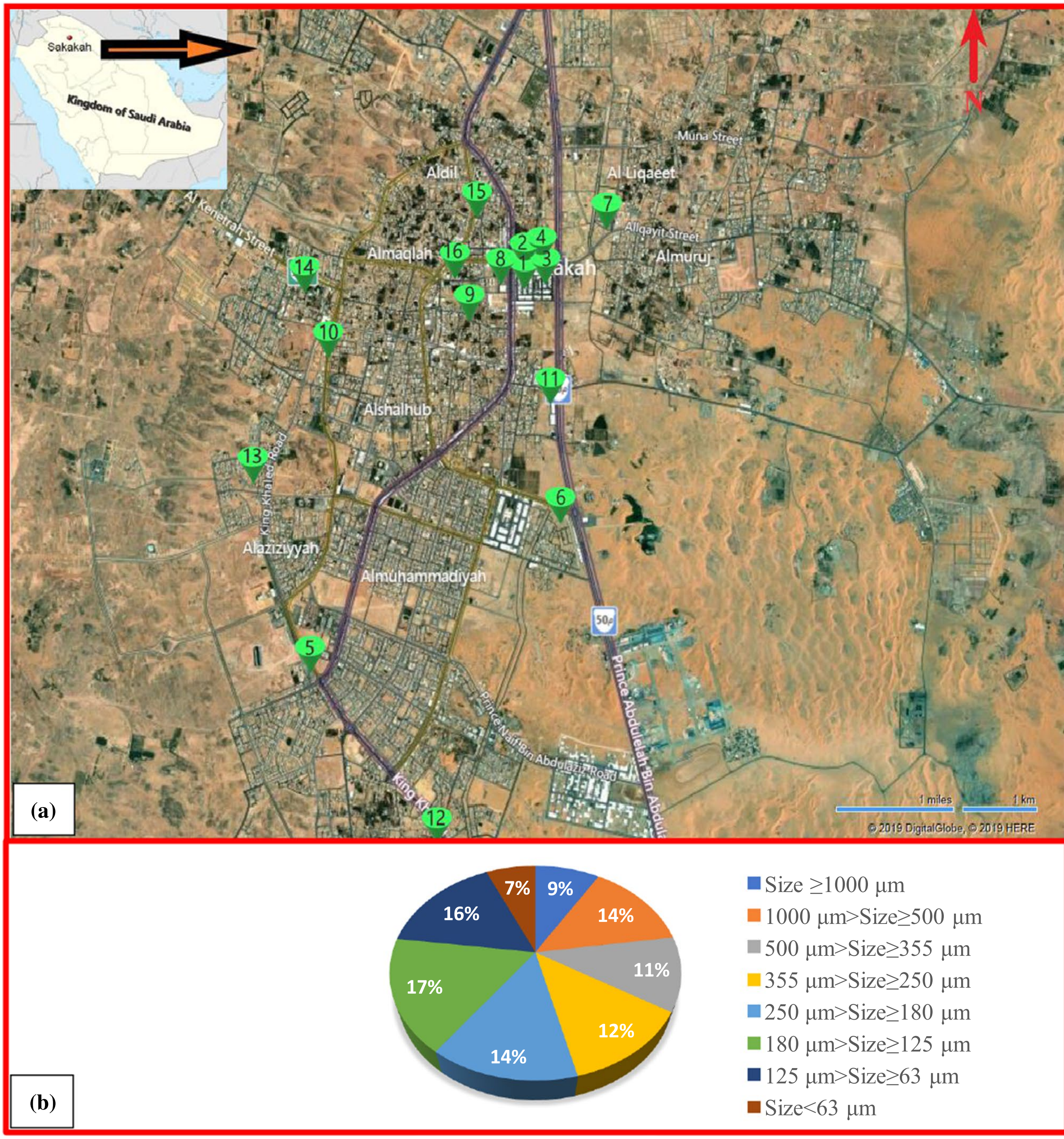

Fig. 1 Map of Sakaka City indicating the road dust sampling sites (**a**) and the average size of all collected road dust samples (**b**)

Statistical Analysis

The statistical and correlation assessment was done using SPSS (version 13.0.; SPSS Inc.). To describe the distribution of trace element levels, parameters of descriptive statistics (maximum, minimum, mean, and standard deviation) were calculated. A variance analysis (ANOVA) with the post hoc Scheffe test was used for average trace elements levels comparison at the distinct studied areas. Differences at probability (p) < 0.05 were regarded to be important statistically. Pearson correlation coefficients have been screened for correlation between trace elements levels. These coefficients of correlation (r) at $p < 0.05$ were regarded statistically important.

Table 1 Description of sampling sites

Site code	Activity	Description
RD1	Small-scale industry	In front of a small workshop for vehicle painting, repairing, and metallic welding
RD2		In front of a small workshop for alumetal manufacturing, such as alumetal kitchens, doors, and windows
RD3		In front of a blacksmith's workshop for production of gates, grilles, railings, light fixtures, furniture, and decorative items
RD4		Located at the exit road to the small-scale industrial area. High traffic area
RD5	Educational and traffic	A parking area located close to college of dentistry. High traffic area
RD6	Commercial	A parking area located close to Othaim supermarket
RD7	Educational	A parking area located close to girl's campus of Jouf University
RD8	Commercial	A parking area located close to Carrefour supermarket
RD9	Commercial and residential	A parking area located at a commercial district. High traffic area
RD10	Hospital	In front of Maternity and Children Hospital and close to roads under repair
RD11	Traffic	Next to a bus station and near to high traffic main road
RD12		Located near to a high traffic main road and in front of a petrol station
RD13	Hospital and residential	In front of health care center surrounded by unpaved roads
RD14	Residential	In front of a mosque. No industrial influence
RD15	Residential and commercial	In front of a mosque and close to traffic intersection
RD16	Educational and residential	Located near city center and close to a school. No industrial influence

Table 2 Limits of detection and quantification for elements measured by ICP-MS. Concentration unit was μg/g

Element	ICP-MS	
	LOD	LOQ
Fe	0.0068	0.0227
Pb	0.0213	0.0709
Se	0.0111	0.0370
As	0.0002	0.0006
Zn	0.0013	0.0044
Cu	0.0011	0.0038
Co	0.0000	0.0001
Mn	0.0003	0.0010
Cr	0.0004	0.0012

Estimation of Pollution Impact

Calculations of enrichment and contamination factors besides pollution load index were carried out to determine the trace elements sources and to recognize the most polluted sites among tested areas.

Enrichment Factor

The anthropogenic source and natural origin can be distinguished by the enrichment factor (EF) estimated by Eq. (1) (Cheng et al. 2018; Loska et al. 2005):

$$\mathrm{EF} = \frac{\left(C_{\mathrm{m}} / C_{\mathrm{ref}} \right)_{\mathrm{sample}}}{\left(C_{\mathrm{m}} / C_{\mathrm{ref}} \right)_{\mathrm{background}}} \quad (1)$$

where C_{m} is the trace metal concentration in RD (mg/kg) and C_{ref} is the reference element concentration (mg/kg).

Contamination Factor and Pollution Load Index

The contamination degree by anthropogenic trace metals was evaluated using contamination factor (Cf). It was estimated by using Eq. (2) (Li et al. 2013):

$$\mathrm{Cf} = \frac{C_{\mathrm{metal}}}{C_{\mathrm{bkg}}} \quad (2)$$

where C_{bkg} is the background trace metal concentration.

However, the pollution load index (PLI) evaluates the pollution degree in the area under investigation from number of trace metals (n) by using Eq. (3) (Tomlinson et al. 1980).

$$\mathrm{PLI} = \left(\mathrm{Cf}_1 \times \mathrm{Cf}_2 \times \mathrm{Cf}_3 \times \cdots \times \mathrm{Cf}_n \right)^{1/n} \quad (3)$$

Health Risk Assessment

It is a method to predict the impacts on health due to exposure to certain chemicals, whether carcinogenic or noncarcinogenic (USEPA 2001).

Average Daily Intake (ADI)

In the current study, health risk assessment was done by calculation of trace elements ADI through ingestion, inhalation, and dermal contact pathways using parameters given in Table 3 for adults and children residents in all study areas beside workers in the small-scale industrial area.

(a) Average ingestion of RD trace elements per day (ADI_{ing}) ($mg\ kg^{-1}\ day^{-1}$) was calculated by Eq. (4) (Aluko, et al. 2018);

$$ADI_{ing} = \frac{C \times IR \times EF \times ED \times CF}{BW \times AT} \quad (4)$$

where C is the trace metal concentration in RD ($mg\ kg^{-1}$), IR is the ingestion rate ($mg\ day^{-1}$), EF is the exposure frequency ($days\ year^{-1}$), ED is the exposure duration (years), BW is the individual weight (kg), AT is the average dose time period (days), and CF is the conversion factor ($kg\ mg^{-1}$).

(b) Average inhalation of trace metals in RD per day (ADI_{inh}) ($mg\ kg^{-1}\ day^{-1}$) was calculated by Eq. (5) (Aluko et al. 2018);

$$ADI_{inh} = \frac{C \times IR_{air} \times EF \times ED}{BW \times AT \times PEF} \quad (5)$$

where IR_{air} is the inhalation rate ($m^3\ day^{-1}$) and PEF is the emission factor of particulate ($m^3\ kg^{-1}$).

(c) Dermal Contact with RD is calculated by Eq. (6) (Aluko et al. 2018);

$$ADI_{dem} = \frac{C \times SA \times FE \times AF \times ABS \times EF \times ED \times CF}{BW \times AT} \quad (6)$$

where ADI_{dem} is the trace metals dermal contact exposure dose ($mg\ kg^{-1}\ day^{-1}$), SA is the skin exposed area (cm^2), FE is the fraction of the dermal exposure to RD, AF is the soil adherence factor ($mg\ cm^{-2}$), and ABS is the applied dose fraction absorbed through skin.

Carcinogenic Risk Assessment

The cancer risk (CR) was evaluated by Eq. (7) (Zhou et al. 2019):

$$CR = ADI_{k\ (ing/inh/der)} \times CSF_k \quad (7)$$

where CR is the probability of cancer over a lifetime and CSF_k is the cancer slope factor (mg/kg/day) taken from official agencies (USEPA 1991, 2007, 2010; Aluko et al. 2018).

The total carcinogenic risk (TR) can be evaluated by Eq. (8) through all of the previous mentioned pathways.

$$Risk_{(total)} = Risk_{(ing)} + Risk_{(inh)} + Risk_{(dermal)} \quad (8)$$

Noncarcinogenic Risk Assessment

It is evaluated by hazard quotient (HQ) value, which is calculated by using Eq. (9) (USEPA 1989).

$$HQ = \frac{ADI}{RfD} \quad (9)$$

where RfD is the chronic reference dose ($mg\ kg^{-1}\ day^{-1}$) taken from official agencies (USEPA 1991, 2007, 2010; Aluko et al. 2018).

Hazard Index (HI) is the summation of HQ for every trace element in the collected RD.

$$HI = \sum_{k=1}^{n} HQk = \sum_{k=1}^{n} \frac{ADI_k}{RfD_k} \quad (10)$$

Table 3 Parameters for risk assessment calculations via various pathways (USEPA 2004)

Parameter	Definition	Unit	Worker	Child	Adult
SA	Skin surface area	cm^2	5800	2100	5800
IR_{air}	Inhalation rate	m^3/day	100	200	100
FE	Dermal exposure ratio	–	0.61	0.61	0.61
AF	Soil adherence factor	mg/cm^2	0.07	0.2	0.07
ABS	Dermal absorption factor	–	0.1	0.1	0.1
EF	Exposure frequency	days/year	330	350	350
ED	Exposure duration	years	42	6	30
PEF	Particulate emission factor	m^3/kg	1.30×10^9	1.30×10^9	1.30×10^9
BW	Body weight	kg	70	15	70
CF	Conversion factor	kg/mg	1.00×10^{-6}	1.00×10^{-6}	1.00×10^{-6}
AT	Average time				
	For carcinogenic assessment		365 × 70	365 × 70	365 × 70
	For noncarcinogenic assessment		365 × ED	365 × ED	365 × ED

where (n) is the number of trace elements.

If HI value is lower than unity, it is improbable that the exposed population will experience any negative health effects, whereas if it exceeds this value, non-carcinogenic impacts are probable to occur (USEPA 1989).

Results and Discussion

RD Size Distribution

Figure 1 shows the average weight percentage of the different size fractions among all collected RD samples. The highest ratio is found to be 17% for size fraction (180–125 µm), and the lowest is 7% for the smallest size fraction (< 63 µm). In agreement with previous studies, the fine-sized fraction of RD almost present in small proportions (Bourliva et al. 2017; Valotto et al. 2018; Lanzerstorfer and Logiewa 2019). The obtained results illustrate that 23% of the RD have size fraction less than 125 µm. In general, the anthropogenic RD pollutants are particularly of fine sizes (Afrifa et al. 2015). This fine-sized fraction of RD (< 100 µm) can easily resuspend into air by vehicles movement or wind blowing more than coarse ones (Wang et al. 2005; El-Hashemy and Nazeer 2016). The fine fraction also is adhered easily to human's skin, especially particles of diameters < 63 µm (Choate et al. 2006), so that the fine RD particles have more harmful impact on health. This work focused on the RD particles of small size mainly less than 63 µm.

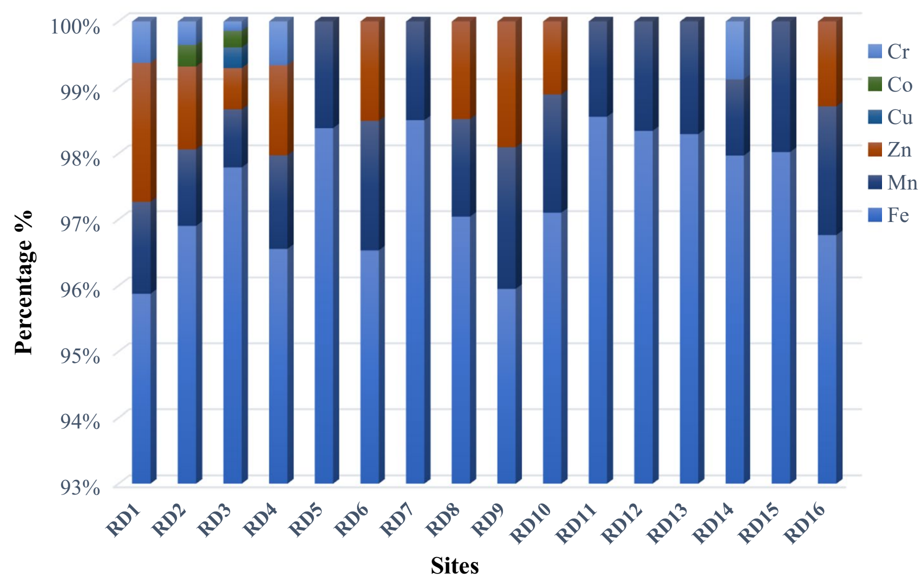

Fig. 2 Concentration distribution of the essential elements obtained by XRF analysis of the collected road dust samples

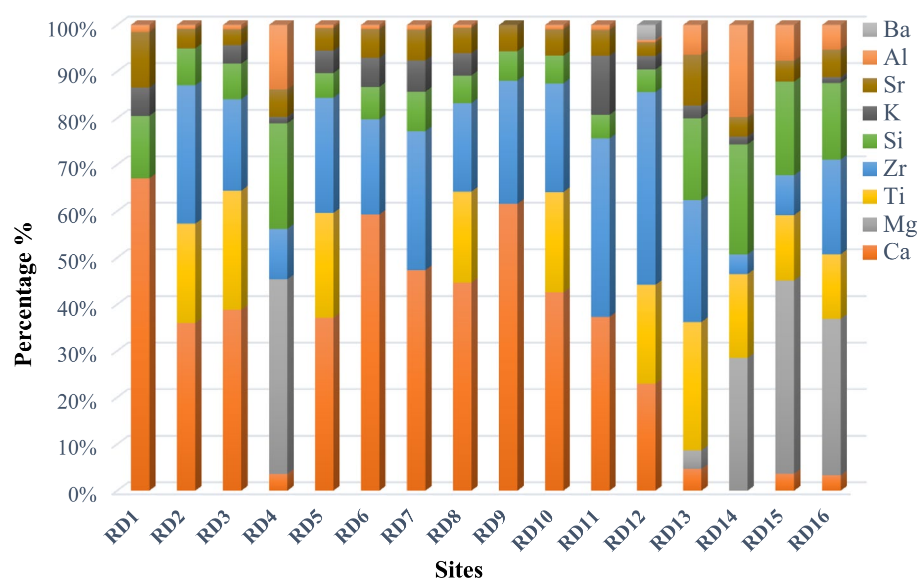

Fig. 3 Concentration distribution of the nonessential elements obtained by XRF analysis of the collected road dust samples

Figures 2 and 3 represent the percentage of the composition of RD particles of size < 63 µm obtained by XRF analysis. Generally, the elements concentration is increased by decreasing particle size of RD except for silicon (Afrifa et al. 2015; Lanzerstorfer and Logiewa 2019). The fine RD particles have higher specific surface area in comparison with coarse ones. Thus, elements of high concentration in the fine-sized fraction may be due to bonding of such elements to the particle surface. The obtained results indicate that there were variations in the concentration of elements from one site to another. This may be attributed to the different activities in each site. For instance, the iron concentration is high in four sites namely (RD1, RD2, RD3, & RD4) due to the presence of small-scale industries which use iron alloys as a raw material.

Trace Metal Content in RD of Particle Size (< 63 µm)

Table 4 shows some statistics related to the contents of nine trace elements in RD of particle size smaller than 63 µm collected from different activity areas. The highest levels of all measured trace elements were recorded at the small-scale industrial area. The average iron level is the highest level among other trace elements. So, it is clear that iron is one of the major elements and most abundant species in urban RD (Ramírez et al. 2019). The concentration values of trace elements are ranked as Fe > Mn > Pb > Zn > Cr > Cu > Co > As > Se. Compared with data obtained from previous studies for other cities, the trace elements measured in RD in Sakaka City are comparable with those determined in both of Ottawa City (Cu, Cr, Zn, and Pb) and Xi'an City (Mn, Co, Cu, Zn, and Pb). However, contents of copper and zinc were less than those in Venice, Delhi, Shanghai, Hsinchu, Manchester, and Kleszczów, although the contents of iron were comparable with those in Hsinchu and Kleszczów (Table 5).

Table 6 mentions the differences between the trace element concentrations in all studied areas and their probability values. A significant difference ($p < 0.05$) is present among the average concentrations of Fe, Mn, Zn, Cu, and Cr measured at low-scale industrial region and all other investigated regions of different activities. Difference in arsenic concentration in the small-scale manufacturing areas and all other investigated areas except hospital areas is significant.

Table 4 Statistical description of element concentrations (µg/g) determined using ICP-MS

Area description		Cr	Mn	Co	Cu	Zn	As	Se	Pb	Fe
Small-scale industrial area $N = 4$	Mean	42.82	400.32	6.21	37.48	103.90	2.43	0.61	114.78	42,942.90
	SD	15.01	138.55	2.61	12.45	17.74	0.98	0.51	71.61	21,182.46
	Max	56.05	543.55	9.55	45.88	124.86	3.82	1.37	220.49	65,875.93
	Min	21.46	218.16	3.70	19.00	81.91	1.56	0.26	65.78	21,246.86
Residential area $N = 5$	Mean	6.72	88.27	1.71	4.15	16.94	0.55	0.22	43.17	3297.78
	SD	2.50	42.34	0.57	2.61	9.30	0.23	0.07	2.85	1255.38
	Max	10.15	158.32	2.13	8.33	31.80	0.80	0.31	46.55	4898.14
	Min	3.62	49.34	0.91	2.19	9.95	0.28	0.12	39.23	1482.65
Hospitals area $N = 2$	Mean	7.99	103.95	2.11	3.63	13.88	0.84	0.29	44.48	4003.42
	SD	2.04	13.64	0.01	1.10	4.59	0.11	0.07	1.12	794.26
	Max	9.43	113.59	2.11	4.41	17.12	0.92	0.34	45.27	4565.05
	Min	6.55	94.30	2.10	2.85	10.63	0.76	0.24	43.69	3441.79
Main roads $N = 3$	Mean	8.51	117.78	2.23	6.20	16.46	0.70	0.33	62.30	4542.04
	SD	4.90	71.66	1.10	2.76	8.33	0.39	0.12	33.40	1999.53
	Max	14.13	199.58	3.46	9.38	26.08	1.13	0.46	100.72	6836.02
	Min	5.15	66.12	1.36	4.58	11.40	0.35	0.22	40.19	3168.45
Commercial area $N = 4$	Mean	10.01	132.54	2.11	8.08	28.17	0.64	0.25	42.31	5277.87
	SD	4.64	57.73	0.80	2.90	6.77	0.50	0.15	2.99	1825.27
	Max	14.58	172.88	2.90	10.85	32.35	1.20	0.43	46.55	6974.49
	Min	5.30	66.42	1.30	5.07	20.37	0.00	0.08	40.06	2872.29
Educational area $N = 3$	Mean	9.05	125.54	2.36	5.54	17.81	0.75	0.31	61.00	4339.04
	SD	5.27	75.15	1.31	3.62	7.36	0.43	0.17	34.43	2694.72
	Max	14.13	199.58	3.46	9.38	26.08	1.13	0.46	100.72	6836.02
	Min	3.62	49.34	0.91	2.19	11.96	0.28	0.12	39.74	1482.65

Table 5 Mean trace elements concentrations (μg/g) in road dust recorded in different countries

City/province	Country	Area	Cr	Mn	Co	Cu	Zn	As	Se	Pb	Fe	References
Venice	Italy	Urban	NA	NA	13	1814	1495	NA	NA	678	NA	Valotto et al. (2015)
Delhi	India	Urban	148.8	NA	NA	192	285	NA	NA	121	NA	Suryawanshi et al. (2016a, b)
Shanghai	China	Urban	159	NA	NA	197	734	NA	NA	295	NA	Shi et al. (2008)
Hsinchu	Taiwan	Urban-industrial	200	490	NA	101	493	NA	19	204	35,900	Wang et al. (2005)
Manchester	UK	Urban	NA	NA	NA	113	653	NA	NA	265	NA	Robertson et al. (2003)
Kleszczów	Poland	Mining area	NA	960	NA	130	440	12	NA	91	61,000	Lanzerstorfer and Logiewa (2019)
Xi'an	China	Urban-residential	172	377	12	48	163	NA	NA	115	NA	Shi and Lu (2018)
Ottawa	Canada	Urban	41.7	NA	NA	38.13	101.3	NA	NA	33.49	NA	Rasmussen et al. (2001)

NA not available

Trace Metal Contamination Assessment

Analysis of EF Values

EF values were calculated using Si as reference element (Shi and Lu 2018) to recognize the trace elements origin whether anthropogenic or natural (Han et al. 2006; Kamani et al. 2015; Zhong et al. 2016; Wang et al. 2016). Figure 4 presents the obtained EF values of trace elements in RD of fraction size < 63 μm. The average EF values were ranked as Pb > Zn > Mn > Fe > Cu > Se > Cr > Co > As. In the small-scale industrial area, the maximum EF value of Pb (40.0) indicates very high enrichment. On the other hand, the maximum EF value of As (1.5) was less than 2 and this demonstrates minimal enrichment, whereas the maximum EF value of Co (3.0) shows moderate enrichment that ranges from 2 to 5. The maximum EF values of Cr (5.2), Cu (8.5), Zn (10.3), Fe (11.6), and Mn (12.0) are between 5 and 20, which shows significant enrichment (Abrahim and Parker 2008). In the other investigated areas, the average EF values were less than unity for all investigated trace elements, except for Se and Pb. Generally, if the EF value is near to 1, the corresponding element has natural origin. But if it exceeds 10, the corresponding element has anthropogenic origin (Han et al. 2006; Zhong et al. 2016; Wang et al. 2016). The calculated EF values confirm the existence of an anthropogenic source for Pb, Zn, Fe, Mn, and Cu. These trace elements in RD have many anthropogenic sources, such as traffic, industry, and construction materials.

Fuel combustion was a source for As, Cr, Fe, and Mn (Suryawanshi et al. 2016a, b; Police et al. 2016; Hsu et al. 2017). Traffic sources include fuel consumption, fuel additives, and vehicle component wear, such as tire wear and debris from brake. Traffic-derived trace elements are Pb, Mn, Cu, Zn, and Fe (Dytłow and Kostrubiec 2019). From literature, Pb was used previously in fuel additives manufacture as tetraethyl lead, which is added to gasoline, but it is forbidden now. Although Pb is no longer a component of traffic exhaust, it still found in wheel weights and brake wear (Grigoratos and Martini 2015). Construction materials besides the metallic materials used in manufacture are considered as Cu source (Jiang et al. 2016; Men et al. 2018).

Analysis of CF and PLI Values

CF is used as a measure of RD trace element contamination degree at the investigated areas. As shown in Fig. 5, the maximum CF values of Mn (1.45), Cu (1.02), Zn (1.89), and Fe (1.40) at small-scale industrial areas are between 1 and 3, which indicates mild contamination. On the other hand, Pb has a maximum CF value (11.02), which refers to very high contamination degree at small-scale industrial areas. The average calculated trace elements CF values have been decreased as follows: Pb > Zn > Mn > Se > Fe > Cu > Cr > Co > As. The average CF values of all trace elements collected from other investigated areas were less than unity except for Pb. The obtained results of CF values confirm the same observations of EF and shows a contamination of RD collected at the small-scale industrial area with Pb, Zn, Mn, Se, Fe, Cu, Cr, Co, and As.

The calculated values of PLI are 0.22, 0.75, 0.16, 0.19, 0.19, and 0.22 for mean roads, industrial, residential, hospitals, commercial, and educational areas, respectively. The highest PLI value recorded at small-scale industrial area (≈ 1) indicates that it is a polluted area.

Correlation Analysis

As shown in Table 7, Pearson's correlation assessment for trace elements is conducted for all studied areas. Strong significant positive correlation is found in RD among only Cr–Mn, Co-As, Pb-As, Co-Pb, and Fe-Cu with $p < 0.05$ at small-scale industrial area. However, at other investigated regions, there is a very strong positive correlation between most of the measured trace elements specially at hospitals areas. The obtained results suggest the accumulation of trace elements from similar sources, such as traffic source at all investigated areas except at small-scale industrial area. The

Table 6 Mean trace element concentration differences between the investigated areas and their *p* values

		Residential area	Hospital	Main roads	Commercial area	Educational areas
Cr						
Industrial area	Mean difference	36.10068*	34.83747*	34.31687*	32.81212*	33.77796*
	Significance level (*p*)	0.000	0.006	0.002	0.003	0.003
Residential area	Mean difference		−1.26321	−1.78381	−3.28856	−2.32272
	Significance level (*p*)		1.000	1.000	0.996	0.999
Hospital	Mean difference			−0.5206	−2.02535	−1.05951
	Significance level (*p*)			1.000	1.000	1.000
Main roads	Mean difference				−1.50475	−0.53891
	Significance level (*p*)				1.000	1.000
Commercial area	Mean difference					0.96584
	Significance level (*p*)					1.000
Mn						
Industrial area	Mean difference	312.04907*	296.36940*	282.54007*	267.77656*	274.78063*
	Significance level (*p*)	0.003	0.029	0.017	0.024	0.02
Residential area	Mean difference		−15.67966	−29.509	−44.27251	−37.26844
	Significance level (*p*)		1	0.998	0.988	0.995
Hospital	Mean difference			−13.82933	−28.59285	−21.58878
	Significance level (*p*)			1	0.999	1
Main roads	Mean difference				−14.76351	−7.75944
	Significance level (*p*)				1	1
Commercial area	Mean difference					7.00407
	Significance level (*p*)					1
Co						
Industrial area	Mean difference	4.49449*	4.1012	3.98095	4.09727	3.84462
	Significance level (*p*)	0.013	0.115	0.07	0.059	0.084
Residential area	Mean difference		−0.39329	−0.51354	−0.39722	−0.64987
	Significance level (*p*)		1	0.998	1	0.995
Hospital	Mean difference			−0.12025	−0.00393	−0.25658
	Significance level (*p*)			1	1	1
Main roads	Mean difference				0.11632	−0.13632
	Significance level (*p*)				1	1
Commercial area	Mean difference					−0.25265
	Significance level (*p*)					1
Cu						
Industrial area	Mean difference	33.32718*	33.84216*	31.27267*	29.39227*	31.93962*
	Significance level (*p*)	0	0.001	0.001	0.001	0.001
Residential area	Mean difference		0.51498	−2.05451	−3.93491	−1.38756
	Significance level (*p*)		1	0.999	0.978	1
Hospital	Mean difference			−2.56949	−4.44989	−1.90254
	Significance level (*p*)			0.999	0.986	1
Main roads	Mean difference				−1.8804	0.66695
	Significance level (*p*)				1	1
Commercial area	Mean difference					2.54735
	Significance level (*p*)					0.998
Zn						
Industrial area	Mean difference	86.95807*	90.02113*	87.43968*	75.72653*	86.08435*
	Significance level (*p*)	0	0	0	0	0
Residential area	Mean difference		3.06306	0.48161	−11.23153	−0.87371
	Significance level (*p*)		1	1	0.84	1
Hospital	Mean difference			−2.58145	−14.2946	−3.93678
	Significance level (*p*)			1	0.83	0.999

Table 6 (continued)

		Residential area	Hospital	Main roads	Commercial area	Educational areas
Main roads	Mean difference				−11.71315	−1.35533
	Significance level (*p*)				0.874	1
Commercial area	Mean difference					10.35782
	Significance level					0.92
As						
Industrial area	Mean difference	1.87289*	1.58292	1.72076*	1.78752*	1.67075*
	Significance level (*p*)	0.006	0.107	0.031	0.013	0.038
Residential area	Mean difference		−0.28997	−0.15214	−0.08537	−0.20214
	Significance level (*p*)		0.994	1	1	0.998
Hospital	Mean difference			0.13783	0.20459	0.08783
	Significance level (*p*)			1	0.999	1
Main roads	Mean difference				0.06676	−0.05001
	Significance level (*p*)				1	1
Commercial area	Mean difference					−0.11677
	Significance level (*p*)					1
Se						
Industrial area	Mean difference	0.38982	0.32183	0.27572	0.35976	0.3015
	Significance level (*p*)	0.428	0.823	0.839	0.566	0.784
Residential area	Mean difference		−0.06799	−0.1141	−0.03006	−0.08832
	Significance level (*p*)		1	0.995	1	0.999
Hospital	Mean difference			−0.04611	0.03793	−0.02033
	Significance level (*p*)			1	1	1
Main roads	Mean difference				0.08404	0.02578
	Significance level (*p*)				0.999	1
Commercial area	Mean difference					−0.05826
	Significance level (*p*)					1
Pb						
Industrial area	Mean difference	71.6055	70.29675	52.48036	72.463	53.77702
	Significance level (*p*)	0.194	0.458	0.627	0.228	0.604
Residential area	Mean difference		−1.30875	−19.12515	0.8575	−17.82848
	Significance level (*p*)		1	0.99	1	0.993
Hospital	Mean difference			−17.8164	2.16625	−16.51973
	Significance level (*p*)			0.997	1	0.998
Main roads	Mean difference				19.98265	1.29667
	Significance level (*p*)				0.99	1
Commercial area	Mean difference					−18.68598
	Significance level (*p*)					0.993
Fe						
Industrial area	Mean difference	39,645.11424*	38,939.47717*	38,400.85780*	37,665.02551*	38,603.86105*
	Significance level (*p*)	0.001	0.012	0.005	0.003	0.004
Residential area	Mean difference		−705.6371	−1244.256	−1980.089	−1041.253
	Significance level (*p*)		1	1	1	1
Hospital	Mean difference			−538.6194	−1274.452	−335.6161
	Significance level (*p*)			1	1	1
Main roads	Mean difference				−735.8323	203.00325
	Significance level (*p*)				1	1
Commercial area	Mean difference					938.83554
	Significance level (*p*)					1

Calculated by one-way ANOVA with Scheffe test

$^{*}p < 0.05$

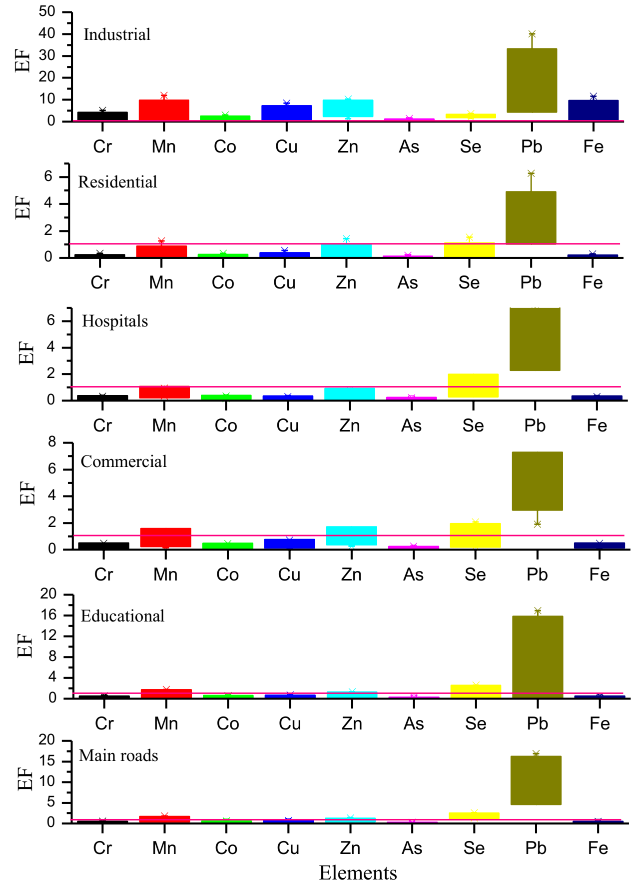

Fig. 4 Box and whisker plots of EF estimated values for trace elements measured in road dust of particle size smaller than 63 µm at the investigated areas

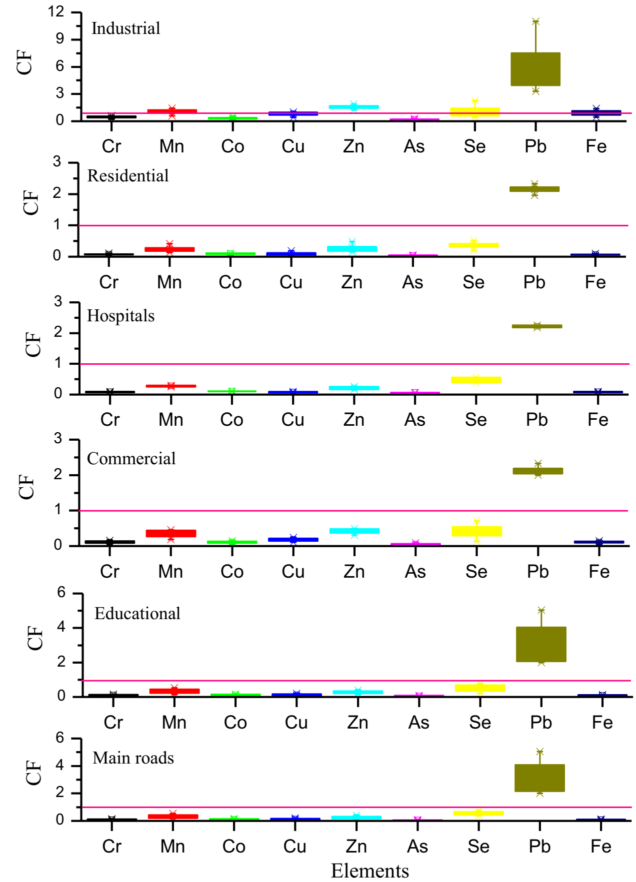

Fig. 5 Box and whisker plots of CF estimated values for trace elements measured in road dust of particle size smaller than 63 µm at the investigated areas

presence of different trace element sources that are related to various industrial activities explains this exception.

Exposure and Health Risk Assessment

Exposure Scenario

The population of Sakaka City is exposed to the toxicity of trace elements that are present in RD due to their outdoor activities. Children are highly affected by the contaminated RD more than adults due to their incomplete safety awareness and their playing habits (Shi et al. 2011; Eqani et al. 2016). At schools and parks, children are not careful to wash their hands before eating food. Moreover, they have a hand-to-mouth behavior and buy street vendor's food that may be contaminated by the polluted RD. One of the tribal traditions in this border region is that people spend their spare time and even celebrations inside tents established in open yards that are exposed to contaminated RD. Workers at the small-scale industrial area spend most of their daytime outdoors in contact with the contaminated RD. Their poor level of health awareness leads to careless behavior, such as eating food in the contaminated work area. This exposure scenario to contaminated RD is supported by the geographical location and weather as Sakaka City is surrounded by a vast desert and characterized by scarcity of rain and frequent sandstorms.

Calculations of health risks resulting from exposure to some trace elements present in road dust have been performed for two population groups of this city under study, namely the category of workers at the small-scale industrial area, and the category of residents in the residential areas of the city, whether adults or children.

Carcinogenic and Noncarcinogenic Risk Assessment

The cancer risk values of Pb, Cr, and Co according to the inhalation pathway are represented in Fig. 6. Furthermore, the cancer risk values of arsenic according to ingestion, inhalation, and dermal pathways also are shown in Fig. 6. The acceptable cancer risk value should be in the range from 1×10^{-6} to 1×10^{-4} according to U.S. Environmental

Table 7 Matrix of Pearson correlation coefficient for RD content of trace elements at the investigated sites

	Cr	Mn	Co	Cu	Zn	As	Se	Pb	Fe		Cr	Mn	Co	Cu	Zn	As	Se	Pb	Fe
Industrial area										Residential area									
Cr	1									Cr	1								
Mn	0.983*	1								Mn	0.876	1							
Co	0.700	0.726	1							Co	0.866	0.676	1						
Cu	−0.151	−0.142	−0.774	1						Cu	0.650	0.836	0.281	1					
Zn	−0.939	−0.977*	−0.598	−0.042	1					Zn	0.577	0.780	0.163	0.990*	1				
As	0.575	0.568	0.965*	−0.895	−0.401	1				As	0.614	0.822	0.619	0.679	0.583	1			
Se	0.129	0.125	0.766	−0.999*	0.056	0.885	1			Se	0.981*	0.879*	0.919*	0.628	0.534	0.725	1		
Pb	0.443	0.447	0.934	−0.948	−0.277	0.988*	0.943	1		Pb	−0.396	−0.081	−0.313	0.173	0.148	0.421	−0.255	1	
Fe	0.501	0.485	−0.249	0.777	−0.610	−0.420	−0.793	−0.554	1	Fe	0.981*	0.872	0.892*	0.668	0.578	0.712	0.996*	−.236	1
Hospitals										Main roads									
Cr	1									Cr	1								
Mn	1.000*	1								Mn	0.999*	1							
Co	1.000*	1.000*	1							Co	0.994	0.997*	1						
Cu	1.000*	1.000*	1.000*	1						Cu	0.993	0.987	0.973	1					
Zn	1.000*	1.000*	1.000*	1.000*	1					Zn	0.990	0.984	0.968	1.000*	1				
As	1.000*	1.000*	1.000*	1.000*	1.000*	1				As	0.968	0.977	0.990	0.930	0.923	1			
Se	1.000*	1.000*	1.000*	1.000*	1.000*	1.000*	1			Se	0.960	0.970	0.985	0.919	0.911	1.000*	1		
Pb	−1.000*	−1.000*	−1.000*	−1.000*	−1.000*	−1.000*	−1.000*	1		Pb	0.980	0.972	0.952	0.997*	0.998*	0.899	0.886	1	
Fe	1.000*	1.000*	1.000*	1.000*	1.000*	1.000*	1.000*	−1.000*	1	Fe	1.000(*)	0.999(*)	0.994	0.992	0.990	0.968	0.961	0.980	1
Commercial area										Educational area									
Cr	1									Cr	1								
Mn	0.932	1								Mn	1.000*	1							
Co	1.000*	0.929	1							Co	0.984	0.978	1						
Cu	0.999*	0.948	0.998*	1						Cu	0.984	0.989	0.938	1					
Zn	0.898	0.996	0.894	0.918	1					Zn	0.942	0.952	0.867	0.986	1				
As	0.988	0.866	0.990	0.980	0.821	1				As	0.989	0.984	1.000*	0.949	0.883	1			
Se	1.000*	0.930	1.000*	0.999*	0.896	0.986*	1			Se	0.994	0.990	0.998*	0.959	0.898	0.999*	1		
Pb	−.981	−.984	−0.980	−0.989	−0.966	−0.008	−0.168	1		Pb	0.814	0.831	0.699	0.903	0.962	0.721	0.744	1	
Fe	0.998*	0.954	0.997*	1.000*	0.925	−0.115	0.039	−0.985*	1	Fe	0.998*	0.996	0.993	0.972	0.920	0.996	0.999*	0.778	1

*Significant at the 0.05 level (2-tailed)

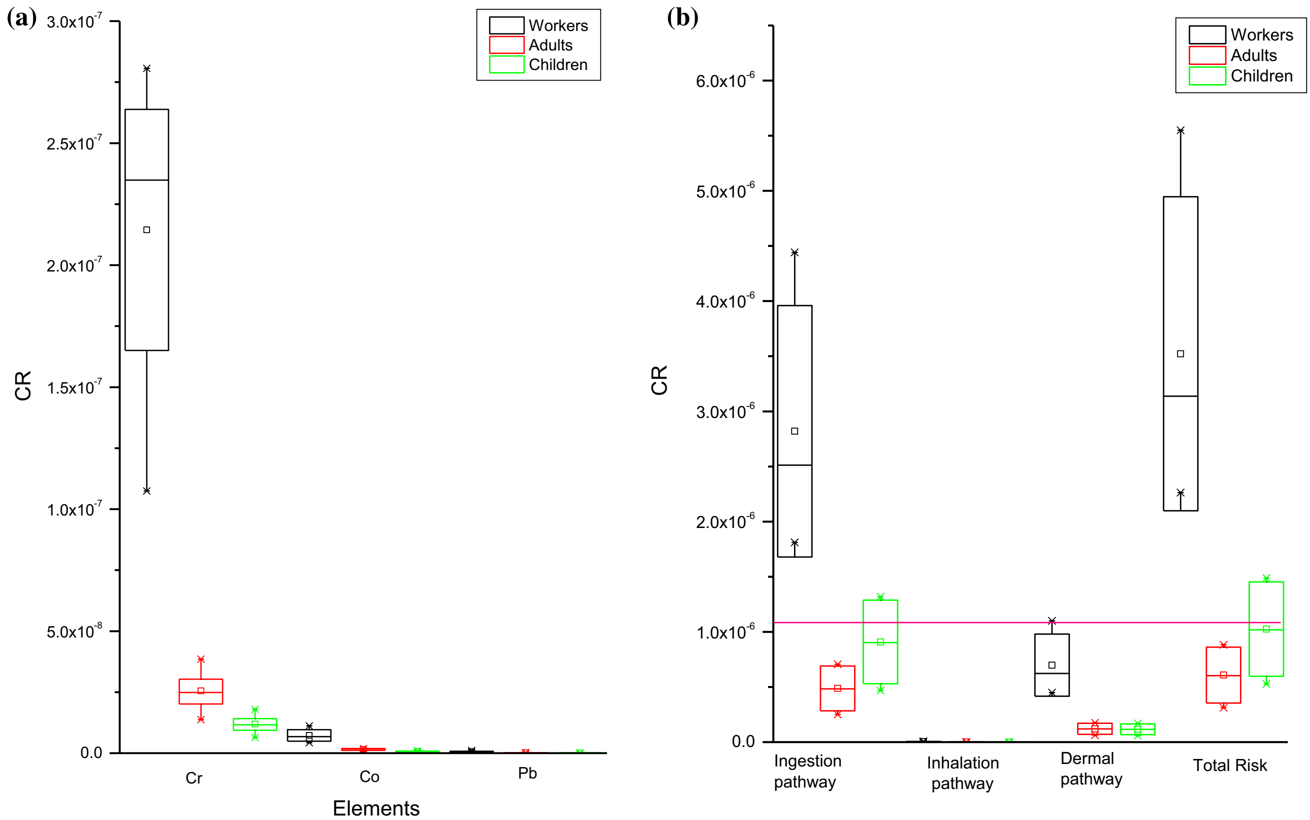

Fig. 6 Carcinogenic risk (CR) of (Cr, Co, Pb) through inhalation pathway (**a**) and that of As in addition to total risk (**b**) for residents (children and adults) and workers

Protection Agency (Zhou et al. 2019). The values of cancer risk for Pb, Cr, and Co were below that range. Arsenic is found to be the leading trace metal to cancer, especially for workers at the small-scale industrial area. The cancer risk values of arsenic for workers (1.8×10^{-6}–4.4×10^{-6}) and resident children (4.7×10^{-7}–1.3×10^{-6}) are found to be $> 1 \times 10^{-6}$ by ingestion pathway, but for adult residents, it was less than this acceptable range. Therefore, workers and resident children are exposed to high risk more than resident adults. It's worth mentioning that the ingestion pathway was the more effective one for cancer risk followed by the dermal contact pathway (4.5×10^{-7}–1.1×10^{-6}), especially for workers at the small-scale industrial area. Consistent with our results, the ingestion is the major pathway for cancer risk in Petaling Jaya (Malysia) (Shabanda et al. 2019).

Total cancer risk values for all investigated trace metals were less than the accepted range except for As. This implies carcinogenic risk as shown in Fig. 6 for both resident children (5.3×10^{-7}–1.5×10^{-6}) and workers (2.3×10^{-6}–5.6×10^{-6}) at the small-scale industrial area.

The results of the ingestion, inhalation, and dermal contact pathways are given as HQ and HI values as illustrated in Fig. 7. If HQ and HI have values lower than unity, the population will not be exposed to risk, but if they become more than unity, potential noncarcinogenic effects become more likely (El-Hashemy and Ali 2018).

The obtained HQ values for iron are lower than unity through inhalation and dermal contact pathways. But this HQ value is more than one through ingestion pathway for all tested groups of population. This indicates very high noncancer risk from iron for both adults and children inhabiting the residential areas and for workers at the small-scale industrial area.

Similar to our results, ingestion is the major pathway for noncancer risk in Shanghai (China) (Shi et al. 2008), Luanda (Angola) (Baptista and De Migue 2005), Hassi Messaoud (Algeria) (Benhaddya et al. 2016), and Pakistan (Eqani et al. 2016).

In general, the ingestion pathway is the major contributor to health risk relative to the inhalation pathway because of the detention of dust particles through nasal pathway (Mohmand et al. 2015). However, HQ and HI values for As, Cr, Cu, Mn, Pb, and Zn as indicated by the three pathways are less than one. This means that the noncarcinogenic risk is neglected for the previous listed metals regarding both workers and residents (adults and children).

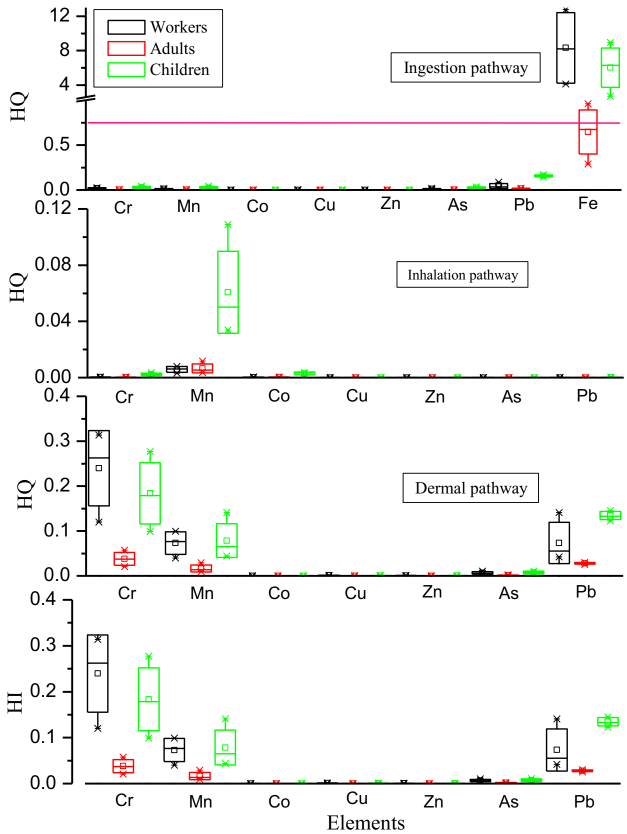

Fig. 7 Box and whisker plots of HQ and HI estimated values for trace elements measured in road dust of particle size smaller than 63 µm for residents (children and adults) and workers

Conclusions

Sakaka City is a small city in a border region and is characterized by the presence of small-scale industries. Our results indicate the diversity of average trace elements concentrations in RD samples of particles size < 63 µm among different areas in this city according to the anthropogenic activities that caused their release. The EF and CF values confirmed the presence of anthropogenic sources for the investigated trace elements. The highest calculated PLI value found at the small-scale industrial area indicates that it is a highly polluted area. There is a strong correlation between most of the detected trace elements at all sites, except at the small-scale industrial area. The variation of the industrial sources of those trace elements explains this exception. There is a noncarcinogenic risk for ingestion of Fe by residents (children and adults) and workers at small-scale industrial area. Both of resident children and workers at small-scale industrial area are more susceptible to carcinogenic risk than adult residents. The trend of contribution to cancer risk shows that the ingestion route is the major one followed by the dermal route. The current evaluation of trace elements levels in RD and related health risk will assist policy makers to make action plans to reduce trace elements that cause pollution in Sakaka City as well as similar cities in the border provinces.

Acknowledgements The authors are grateful to the chemistry department at Jouf University for giving the access to conduct this work. The authors extend also their appreciation to the central laboratory, Jouf University for performing analysis.

References

Abdel-Latif N, Saleh I (2012) Heavy metals contamination in roadside dust along major roads and correlation with urbanization activities in Cairo, Egypt. J Am Sci 8(6):379–389

Abrahim G, Parker R (2008) Assessment of heavy metal enrichment factors and the degree of contamination in marine sediments from Tamaki Estuary, Auckland, New Zealand. Environ Monit Assess 136:227–238

Afrifa C, Ofosu F, Bamforf S, Atiemo S, Aboh I, Gyampo O, Ahiamadjie H, Adeti J, Arthur J (2015) Health risk assessment of heavy metal exposure from soil dust at selected fuel filling stations in Accra. Int J Sci Technol 4(7):289–296

Ahmad I, Balkhyour MA, Abokhashabah TM, Ismail IM, Rehan M (2017) Workplace safety and health conditions and facilities in small industries in Jeddah, Saudi Arabia. J Safety Study 3:37–52

Al-Dabbous A, Khan A, Al-Rashidi M, Awadi L (2013) Carbon dioxide and volatile organic compounds levels in mosque in hot arid climate. Indoor Built Environ 22(2):456–464

Aluko TS, Njoku KL, Adesuyi AA, Akinola MO (2018) Health risk assessment of heavy metals in soil from the iron mines of Itakpe and Agbaja, Kogi State, Nigeria. Pollution 4(3):527–538

Apeagyei E, Bank M, Spengler J (2011) Distribution of heavy metals in road dust along an urban-rural gradient in Massachusetts. Atmos Environ 45(13):2310–2323

Balkhyour M, Ahmad I, Rehan M (2019) Assessment of personal protective equipment use and occupational exposures in small industries in Jeddah: health implications for workers. Saudi J Biol Sci 26:653–659

Baptista L, De Migue E (2005) Geochemistry and risk assessment of street dust in Luanda, Angola: a tropical urban environment. Atmos Environ 39:4501–4512

Benhaddya M, Boukhelkhal A, Halis Y, Hadjel M (2016) Human health risks associated with metals from urban soil and road dust in an oilfield area of southeastern Algeria. Arch Environ Contam Toxicol 70:556–571

Bourliva A, Christophoridis C, Papadopoulou L, Giouri K, Papadopoulos A, Mitsika E, Fytianos K (2017) Characterization, heavy metal content and health risk assessment of urban road dusts from the historic center of the city of Thessaloniki, Greece. Environ Geochem Health 39:611–634

Cao Z, Zhao L, Kuang J, Chen Q, Zhu G, Zhang K, Wang S, Wu P, Zhang X, Wang X, Harrad S, Sun J (2017) Vehicles as outdoor BFR sources: evidence from an investigation of BFR occurrence in road dust. Chemosphere 179:29–36

Cheng Z, Chen LJ, Li HH, Lin JQ, Yang ZB, Yang YX, Xu XX, Xian JR, Shao JR, Zhu XM (2018) Characteristics and health risk assessment of heavy metals exposure via household dust from urban area in Chengdu, China. Sci Total Environ 619:621–629

Choate L, Ranville J, Bunge A, Macalady D (2006) Dermally adhered soil: 1. Amount and particle-size distribution. Int Environ Assess Manag 2:375–384

Cook AG, Weinstein P, Centeno JA (2005) Health effects of natural dust. Biol Trace Elem Res 103(1):1–15

Dytłow S, Kostrubiec B (2019) Effective and universal tool for evaluating heavy metals: passive dust samplers. Environ Pollut 247:188–194

Eaton AD, Clesceri LS, Greenberg AE (1995) Standard methods for the examination of water and wastewater, 19th edn. American Public Health Association, Washington DC

El-Hashemy M, Ali H (2018) Characterization of BTEX group of VOCs and inhalation risks in indoor microenvironments at small enterprises. Sci Total Environ 645:974–983

El-Hashemy M, Nazeer A (2016) Impact of soil and air contaminants on the composition of rail-head surface rust. Anti Corros Methods Mater 63(2):116–127

Eqani S, Kanwal A, Bhowmik A, Sohail M, Ullah R, Ali S, Alamdar A, Ali N, Fasola M, Shen H (2016) Spatial distribution of dust-bound trace elements in Pakistan and their implications for human exposure. Environ Pollut 213:213–222

Grigoratos T, Martini G (2015) Brake wear particle emissions: a review, 2015. Environ Sci Pollut Res 22:2491–2504

Han Y, Du P, Cao J, Posmentier ES (2006) Multivariate analysis of heavy metal contamination in urban dusts of Xi'an Central China. Sci Total Environ 355:176–186

Hsu CY, Chiang HC, Chen MJ, Chuang CY, Tsen CM, Fang GC, Tsai YI, Chen NT, Lin TY, Lin SL (2017) Ambient $PM_{2.5}$ in the residential area near industrial complexes: spatiotemporal variation, source apportionment, and health impact. Sci Total Environ 590–591:204–214

Jiang Y, Chao S, Liu J, Yue Y, Chen Y, Zhang A, Cao H (2016) Source apportionment and health risk assessment of heavy metals in soil for a township in Jiangsu Province, China. Chemosphere 168:1658–1668

Kamani H, Ashrafi SD, Isazadeh S, Jaafari J, Hoseini M, Mostafapour FK, Bazrafshan E, Nazmara S, Mahvi AH (2015) Heavy metal contamination in street dusts with various land uses in Zahedan, Iran. Bull Environ Contam Toxicol 94:382–386

Khanal R, Furumai H, Nakajima F (2015) Characterization of toxicants in urban road dust by toxicity identification evaluation using ostracod Heterocypris incongruens direct contact test. Sci Total Environ 530–531:96–102

Khanal R, Furumai H, Nakajima F, Yoshimura C (2018) Carcinogenic profile, toxicity and source apportionment of polycyclic aromatic hydrocarbons accumulated from urban road dust in Tokyo, Japan. Ecotoxicol Environ Saf 165:440–449

Kumar P, Gayathri R (2009) Adsorption of Pb^{2+} ions from aqueous solutions onto bael tree leaf powder: isotherms, kinetics and thermodynamics study. J Eng Sci Technol 4:381–399

Lanzerstorfer C, Logiewa A (2019) The upper size limit of the dust samples in road dust heavy metal studies: benefits of a combined sieving and air classification sample preparation procedure. Environ Pollut 245:1079–1085

Li G, Hu B, Bi J, Leng Q, Xiao C, Yang Z (2013) Heavy metals distribution and contamination in surface sediments of the coast-al Shandong Peninsula (Yellow Sea). Mar Pollut Bull 76(1–2):420–426

Liang S, Cui J, Bi X, Luo X, Li X (2019) Deciphering source contributions of trace metal contamination in urban soil, road dust, and foliar dust of Guangzhou, southern China. Sci Total Environ 695:133596

Loska K, Wiechuła D, Pelczar J (2005) Application of enrichment factor to assessment of zinc enrichment/depletion in farming soils. Commun Soil Sci Plant Anal 36(9–10):1117–1128

Men C, Liu R, Wang Q, Guo L, Shen Z (2018) The impact of seasonal varied human activity on characteristics and sources of heavy metals in metropolitan road dusts. Sci Total Environ 637–638:844–854

Mohmand J, Eqani S, Fasola M, Alamdar A, Ali N, Mustafa I, Liu P, Peng S, Shen H (2015) Human exposures to toxic metals via contaminated dust: bioaccumulation trends and risk assessment. Chemosphere 132:142–151

Offenberg JH, Eisenreich SJ, Chen LC, Cohen MD, Chee G, Prophete C, Weisel C, Lioy PJ (2003) Persistent organic pollutants in the dusts that settled across lower Manhattan after September 11, 2001. Environ Sci Technol 37:502–508

Police S, Sahu SK, Pandit GG (2016) Chemical characterization of atmospheric particulate matter and their source apportionment at an emerging industrial coastal city, Visakhapatnam, India. Atmos Pollut Res 7:725–733

Rahman M, Khan M, Jolly Y, Kabir J, Akter S, Salam A (2019) Assessing risk to human health for heavy metal contamination through street dust in the Southeast Asian Megacity: Dhaka, Bangladesh. Sci Total Environ 660:1610–1622

Ramírez O, Sánchez A, Amato F, Moreno T, Silva L, Rosa J (2019) Physicochemical characterization and sources of the thoracic fraction of road dust in a Latin American megacity. Sci Total Environ 652:434–446

Rasmussen P, Subramanian S, Jessiman B (2001) A multi-element profile of house dust in relation to exterior dust and soils in the city of Ottawa, Canada. Sci Total Environ 267:125–140

Robertson D, Taylor K, Hoon S (2003) Geochemical and mineral magnetic characterization of urban sediment particulates, Manchester, UK. Appl Geochem 18(2):269–282

Seneviratne M, Phoon WO (2006) Exposure assessment in SMEs: a low-cost approach to bring OHS services to small-scale enterprises. Ind Health 44:27–30

Shabanda I, Koki I, Low K, Zain S, Khor S, Bakar N (2019) Daily exposure to toxic metals through urban road dust from industrial, commercial, heavy traffic, and residential areas in Petaling Jaya, Malaysia: a health risk assessment. Environ Sci Pollut Res 26(36):37193–37211

Shabbaj I, Alghamdi M, Shamy M, Hassan S, Alsharif M, Khoder M (2018) Risk assessment and implication of human exposure to road dust heavy metals in Jeddah, Saudi Arabia. Int J Environ Res Public Health 15:36

Shi D, Lu X (2018) Accumulation degree and source apportionment of trace metals in smaller than 63 μm road dust from the areas with different land uses: a case study of Xi'an, China. Sci Total Environ 636:1211–1218

Shi G, Chen Z, Xu S, Zhang J, Wang L, Bi C, Teng J (2008) Potentially toxic metal contamination of urban soils and roadside dust in Shanghai, China. Environ Pollut 156:251–260

Shi G, Chen Z, Bi C, Wang L, Teng J, Li Y, Xu S (2011) Comparative study of health risk of potentially toxic metals in urban and suburban road dust in the most populated city of China. Atmos Environ 45(3):764–771

Shyam R, Puri J, Kaur H, Amutha R, Kapila A (2013) Single and binary adsorption of heavy metals on fly ash samples from aqueous solution. J Mol Liquid 178:31–36

Sun C, Bi C, Chen Z, Wang D, Zhang C, Sun Y, Yu Z, Zhou D (2010) Assessment on environmental quality of heavy metals in agricultural soils of Chongming Island, Shanghai City. J Geogr Sci 20(1):135–147

Suryawanshi P, Rajaram B, Bhanarkar A, Chalapatirao C (2016a) Determining heavy metal contamination of road dust in Delhi, India. Atmósfera 29(3):221–234

Suryawanshi S, Chauhan AS, Verma R, Gupta T (2016b) Identification and quantification of indoor air pollutant sources within a residential academic campus. Sci Total Environ 569–570:46–52

Tomlinson DL, Wilson JG, Harris CR, Jeffrey DW (1980) Problems in the assessment of heavy-metal levels in estuaries and the formation of a pollution index. Helgolander Meeresuntersuchungen 33:566–575

U.S. Environmental Protection Agency (1989) Risk assessment guidance for superfund volume 1: human health evaluation manual (part A). Office of Emergency and Remedial Response, Washington, DC

U.S. Environmental Protection Agency (1991) Human health evaluation manual, supplemental guidance: standard default exposure factors. USEPA, Washington, DC

U.S. Environmental Protection Agency (2001) Toxics release inventory: public data release report. USEPA, Washington, DC

U.S. Environmental Protection Agency (2004) Risk assessment guidance for superfund volume I: human health evaluation manual (part E, supplemental guidance for dermal risk assessment). USEPA, Washington, DC

U.S. Environmental Protection Agency (2007) Framework for determining a mutagenic mode of action for carcinogenicity: review draft

U.S. Environmental Protection Agency (2010) Recommended use of BW3/4 as the default method in derivation of the oral reference dose

Valko M, Rhodes C, Moncol J, Izakovic M, Mazur M (2006) Free radicals, metals and antioxidants in oxidative stress-induced cancer. Chem Biol Interact 160(1):1–40

Valotto G, Rampazzo G, Visin F, Gonella F, Cattaruzza E, Glisenti A, Formenton G, Tieppo P (2015) Environmental and traffic-related parameters affecting road dust composition: a multi-technique approach applied to Venice area (Italy). Atmos Environ 122:596–608

Valotto G, Zannoni D, Rampazzo G, Visin F, Formenton G, Gasparello A (2018) Characterization and preliminary risk assessment of road dust collected in Venice airport (Italy). J Geochem Explor 190:142–153

Vardhan K, Kumar P, Panda R (2019) A review on heavy metal pollution, toxicity and remedial measures: current trends and future perspectives. J Mol Liquids 290:111197

Wang C, Chang C, Tsai S, Chiang H (2005) Characteristics of road dust from different sampling sites in Northern Taiwan. J Air Waste Manag Assoc 55(8):1236–1244

Wang Q, Lu X, Pan H (2016) Analysis of heavy metals in the resuspended road dust from different functional areas in Xi'an, China. Environ Sci Pollut Res 23:19838–19846

Yu L, Wang G, Zhang R, Zhang L, Song Y, Wu B, Li X, An K, Chu J (2013) Characterization and source apportionment of PM2.5 in an urban environment in Beijing. Aerosol Air Qual Res 13:574–583

Zheng G, Yue L, Li Z, Chao C (2006) Assessment on heavy metals pollution of agricultural soil in Guanzhong district. J Geogr Sci 16(1):105–113

Zheng N, Liu J, Wang Q, Liang Z (2010) Health risk assessment of heavy metal exposure to street dust in the zinc smelting district, northeast of China. Sci Total Environ 408(4):726–733

Zhong C, Yang Z, Jiang W, Hu B, Hou Q, Yu T, Li J (2016) Ecological geochemical assessment and source identification of trace elements in atmospheric deposition of an emerging industrial area: Beidu Gulf economic zone. Sci Total Environ 573:1519–1526

Zhou L, Liu G, Shen M, Hu R, Sun M, Liu Y (2019) Characteristics and health risk assessment of heavy metals in indoor dust from different functional areas in Hefei, China. Environ Pollut 251:839–849